Robust PID Load Frequency Controller Design with Specific Gain and Phase Margin for Multi-area Power Systems

Jitendra Sharma*, Yogesh V. Hote, Rajendra Prasad†**

*Electrical Engineering Department, Indian Institute of Technology, Roorkee, INDIA (e-mail: jitendra13.pj@gmail.com).
**Electrical Engineering Department, Indian Institute of Technology, Roorkee, INDIA (e-mail: yhotefee@iitr.ac.in).
† Electrical Engineering Department, Indian Institute of Technology, Roorkee, INDIA (e-mail: rpdeefee@iitr.ac.in).

Abstract: In interconnected power systems, the load frequency control (LFC) is considered a hugely beneficial ancillary service. The goal of the LFC in an interconnected power system is to limit the frequency of each area within certain bounds and to maintain the tie-line power flows within some pre-specified latitudes by balancing the power outputs of the generators so as to satisfy ever changing load demands. In the classical control theory, PID controller is said to be robust if it provides some specific gain and phase margin. In this paper, a novel methodology is proposed for the robust PID controller design having specific gain and phase margins for LFC in a multi-area power system. The proposed technique is based on stability boundary locus and PID controllers are designed for four-area power system having different types of turbines. The simulations are carried out using MATLAB and effectiveness of the proposed methodology is verified by the comparison with a recently published approach.

Keywords: Load frequency control, multi-area power system, PID controller, specific gain and phase margin, stability boundary locus.

1. INTRODUCTION

For the power system to be operated satisfactorily, the frequency should remain almost constant. The constant frequency enables consistent speed of synchronous and induction motors. The frequency of a system depends on the balance of active power. Since frequency is a common component everywhere in the system, a deviation in the active power demand at one point is echoed all over the system by a deviation in frequency. In an interconnected system having more than one independent control areas, frequency as well as power generation inside each area has to be regulated so as to uphold the scheduled power interchange. The control of frequency and generation is frequently mentioned as load frequency control (LFC) (Kundur, 1994).

LFC is an active area of research now-a-days. A PID controller design scheme based on the direct synthesis (DS) approach in frequency domain is presented by (Anwar & Pan, 2015). An observer based integral sliding surface is developed and a sliding mode LFC (SMLFC) controller is suggested for minimizing the frequency changes in wind power systems by (Cui et al., 2017). In (Guha et al., 2016), LFC problem has been explained in a multi-area power system where PI/PID controllers are tuned using grey wolf optimization (GWO) approach. In (Hussein et al., 2017), Proportional-Integral-Observer (PI-Observer) based state feedback controller has been synthesized for LFC problem of a single area isolated power system model. (Padhan & Majhi, 2013) estimated the power system dynamics using relay based identification technique and then a PID controller is designed for the LFC problem of single and multi-area power systems where PID controller gain parameters are acquired by enlarging the controller transfer function using Laurent series. (Prasad et al., 2017) tackled LFC problem in three area power system using nonlinear sliding mode controller (SMC) with matched and unmatched uncertainties and the proposed approach is validated on IEEE 39 bus power system. The neural network based integral sliding mode controller is used for LFC problem for nonlinear power systems with wind turbines by (Qian et al., 2016). A tilt-integral-derivative controller with filter (TIDF) is designed for LFC problem of multi-area power systems by (Sahu et al., 2016) in which TIDF controller parameters has been optimized by Differential Evolution (DE) algorithm.

A two degree of freedom internal model control (IMC) filter is designed for the LFC problem by (Saxena & Hote, 2013) in which the proposed control strategy is implemented on the reduced order model of the single-area power system. In (Saxena & Hote, 2017), IMC approach is used for the stabilization of perturbed LFC single-area and multi-area power systems and the proposed technique is further validated on the standard IEEE 39 bus system. In (Shayeghi et al., 2008), LFC problem has been solved in a restructured power system by implementing a particle swarm optimization based multi-staged fuzzy (PSOMSF) controller. In (Sondhi & Hote, 2016), a fractional order PID controller has been synthesized by taking the perturbed model of the single-area

LFC utilizing the Kharitonov's theorem. In (Tan, 2009; Tan, 2010), PID controllers are tuned for LFC problem of single-area and multi-area power systems using two-degree-of-freedom IMC technique. A novel robust LFC methodology has been suggested which considers the unmodeled dynamics of power systems by (Tan & Xu, 2009), furthermore, a new arrangement is also presented to outdo the consequences of generation rate constraints (GRC). Discrete-time sliding mode controller has been designed for handling the LFC problem in power system control areas by (Vrdoljak et al., 2010).

The PID controller is widely used in various industries because of its simplicity and availability of various methods of its tuning e.g., Ziegler-Nichols method, Cohen-Coon method, Chien-Hrones-Reswick (CHR) method, IMC technique, stability boundary locus (SBL) method etc. In (Tan et al., 2006), a methodology for designing the stabilizing PI and PID controllers has been given by using the SBL approach, furthermore, the proposed technique is extended for achieving user specified gain and phase margin and for designing PID controllers for interval systems. Robust PI controller is synthesized utilizing the SBL technique for an unstable continuous stirred tank reactor (CSTR) system with parametric uncertainty by (Zavacka et al., 2012). One joint robotic arm has been stabilized by a PI controller using SBL technique for desired gain and phase margin by (Hote, 2016). In (Deniz et al., 2016), an integer order approximation procedure has been proposed for the numerical realization of fractional order integration and differentiation operations in control systems. In (Sonmez & Ayasun, 2016), the stabilizing PI controller parameters has been calculated for a single-area LFC system with time delay. In (Saxena & Hote, 2016), PID controllers have been designed for LFC issues of multi-area power systems using SBL approach.

In this paper, a graphical approach of PID controller tuning known as stability boundary locus (SBL) approach to handle the LFC problem of a four-area power system is used. The advantage of SBL approach is that it does not involve linear programming to crack the inequalities and there is no need of sweeping over the parameters (Tan et al., 2006). The uniqueness of this paper is that the controllers are designed for specific gain margin and specific phase margin.

The remaining paper is arranged as follows. In Section 2, the modeling of load frequency control is given. The proposed technique of PID controller design using SBL for specific gain and phase margin is described in Section 3. Simulation results are discussed in Section 4, and then finally conclusion is stated in Section 5.

2. MODELING OF LOAD FREQUENCY CONTROL

The Electric power systems are highly complex and nonlinear in nature. However, in normal operating conditions these power systems are subjected to small load changes. Therefore, a linearized model of the load frequency control (LFC) is used in interconnected power systems (Saxena & Hote, 2016). The i th control area of a multi-area power system is shown in Fig. 1. The mathematical models of governor, $P_{G,i}(s)$, and load and machine, $P_{LM,i}(s)$, are given by

$$P_{G,i}(s)=\frac{1}{sT_G+1} \tag{1}$$

$$P_{LM,i}(s)=\frac{K_P}{sT_P+1} \tag{2}$$

where, T_G, K_P, and T_P are the governor time constant, electric system (load and machine) gain, and electric system time constant respectively.

$P_{T,i}(s)$ is the turbine transfer function for the i th control area which can be a non-reheated thermal, reheated thermal, or a hydro turbine. The dynamical models for the i th control area of non-reheated, $P_{NRT,i}(s)$, reheated, $P_{RT,i}(s)$, and hydro, $P_{HT,i}(s)$ turbines are described by the transfer functions represented as

$$P_{NRT,i}(s)=\frac{1}{sT_T+1} \tag{3}$$

$$P_{RT,i}(s)=\frac{scT_R+1}{(sT_T+1)(sT_R+1)} \tag{4}$$

$$P_{HT,i}(s)=\frac{-T_W s+1}{0.5T_W s+1} \tag{5}$$

where, T_T, T_R, and T_W are the time constants of the non-reheated thermal turbine, reheated thermal turbine, and hydro turbine respectively and c is the fraction of power generated in the reheat section of the reheated thermal turbine.

The transfer function of the LFC system having non-reheated turbine with droop characteristics (R) is given by

$$G_{NRTD,i}(s)=\frac{P_{G,i}(s)P_{NRT,i}(s)P_{LM,i}(s)}{1+P_{G,i}(s)P_{NRT,i}(s)P_{LM,i}(s)/R} \tag{6}$$

which is equivalent to

$$G_{NRTD,i}(s)=\frac{b_0}{a_0s^3+a_1s^2+a_2s+a_3} \tag{7}$$

where, $b_0=K_P$, $a_0=T_GT_TT_P$, $a_1=(T_GT_T+T_TT_P+T_PT_G)$, $a_2=(T_G+T_T+T_P)$, and $a_3=\left(1+\frac{K_P}{R}\right)$.

The transfer function of the LFC system having non-reheated turbine without droop characteristics is given by

$$G_{NRT,i}(s)=P_{G,i}(s)P_{NRT,i}(s)P_{LM,i}(s) \tag{8}$$

which is equivalent to

$$G_{NRT,i}(s)=\frac{b_0}{a_0s^3+a_1s^2+a_2s+1} \tag{9}$$

where, b_0, a_0, a_1, and a_2 are the same as defined in (7).

The transfer function of the LFC system having reheated turbine without droop characteristics is given by

$$G_{RT,i}(s)=P_{G,i}(s)P_{RT,i}(s)P_{LM,i}(s) \tag{10}$$

which is equivalent to

$$G_{RT,i}(s)=\frac{n_0s+n_1}{m_0s^4+m_1s^3+m_2s^2+m_3s+1} \tag{11}$$

where, $n_0=cT_RK_P$, $n_1=K_P$, $m_0=T_GT_TT_PT_R$, $m_1=(T_PT_GT_T+T_PT_GT_R+T_TT_RT_P+T_TT_RT_G)$,

$m_2 = \left(T_P T_T + T_P T_R + T_G T_T + T_G T_R + T_P T_G + T_T T_R\right)$, and
$m_3 = \left(T_P + T_G + T_T + T_R\right)$.

The transfer function of the LFC system having hydro turbine without droop characteristics is given by

$$G_{HT,i}(s) = P_{G,i}(s) P_{HT,i}(s) P_{LM,i}(s) \tag{12}$$

which is equivalent to

$$G_{HT,i}(s) = \frac{q_0 s + q_1}{p_0 s^3 + p_1 s^2 + p_2 s + 1} \tag{13}$$

where, $q_0 = -K_P T_W$, $q_1 = K_P$, $p_0 = 0.5 T_P T_G T_W$, $p_1 = \left(T_P T_G + 0.5 T_P T_W + 0.5 T_G T_W\right)$, and $p_2 = \left(T_P + T_G + 0.5 T_W\right)$.

3. PID CONTROLLER DESIGN USING SBL

Consider a load frequency control (LFC) system of an i th control area of a multi-area power system as shown in Fig. 1, in which the change in frequency $\left(\Delta f_i\right)$ and net tie-line power interchange $\left(\Delta P_{tie,i}\right)$ is regulated against the change in load disturbance $\left(\Delta P_{d,i}\right)$.

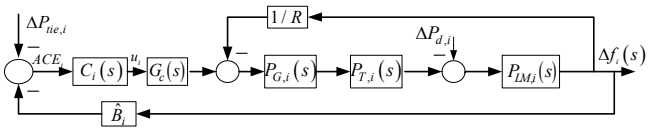

Fig.1. Load frequency control system

In the load frequency control of multi-area power systems, the frequency of each area as well as the net power interchange via the tie-lines should return to their nominal values. Therefore, a combined estimate, known as area control error (ACE) is used as the feedback signal. For the i th control area, the ACE_i is defined as

$$ACE_i = -\left(\hat{B}_i \Delta f_i + \Delta P_{tie,i}\right) \tag{14}$$

where, $\hat{B}_i$ and Δf_i is the frequency bias factor and the frequency deviation of the i th control area respectively and $\Delta P_{tie,i}$ is the net tie-line power interchange among the i th control area and the other control areas. For a power system having M control areas, the total tie-line power interchange among i th control area and other areas is given by

$$\sum_{\substack{j=1 \\ j \neq i}}^{M} \Delta P_{tie,ij}(s) = \frac{2\pi}{s}\left[\sum_{\substack{j=1 \\ j \neq i}}^{M} T_{ij} \Delta f_i(s) - \sum_{\substack{j=1 \\ j \neq i}}^{M} T_{ij} \Delta f_j(s)\right] \tag{15}$$

where, T_{ij} is the synchronizing constant between i th and j th control area.

The control input for the i th control area then becomes,

$$u_i = C_i(s)\, ACE_i \tag{16}$$

where, $C_i(s)$ is the PID controller of the i th control area, given by

$$C_i(s) = \left(k_p + \frac{k_i}{s} + s k_d\right) \tag{17}$$

where, k_p, k_i, and k_d are the proportional, integral and derivative gains of the PID controller. The PID controller parameters can be obtained by using the SBL approach having specific gain and phase margin for power system having different types of turbines as given in the following sub-sections.

3.1 Non-reheated Turbine with Droop Characteristics

The closed loop characteristic equation for the system is given by

$$1 + C_i(s) G_c(s) G_{NRTD,i}(s) = 0 \tag{18}$$

$$1 + \left(k_p + \frac{k_i}{s} + s k_d\right)\left(A e^{-j\phi}\right)\left(\frac{b_0}{a_0 s^3 + a_1 s^2 + a_2 s + a_3}\right) = 0 \tag{19}$$

where, $G_c(s) = A e^{-j\phi}$ is the transfer function of the gain phase margin tester (a virtual compensator) in which A and ϕ are the minimum specific gain and phase margin respectively. These specific gain and phase margins are the measure of the robustness of the system since the PID controller designed by cascading the $G_c(s)$ in the control loop will provide gain margin and phase margin at least equal to A, and ϕ respectively.

Substituting $e^{-j\phi} = \left(\cos\phi - j\sin\phi\right)$ in (19) and then simplifying, results in the following

$$\begin{aligned} &a_0 s^4 + a_1 s^3 + \left(a_2 + b_0 A k_d \cos\phi - j b_0 A k_d \sin\phi\right) s^2 \\ &+ \left(a_3 + b_0 A k_p \cos\phi - j b_0 A k_p \sin\phi\right) s \\ &+ \left(b_0 A k_i \cos\phi - j b_0 A k_i \sin\phi\right) = 0 \end{aligned} \tag{20}$$

Now, putting $s = j\omega$ in (20) and equating the real and imaginary parts of resulting equation to zero, yields

$$k_p = \frac{\left(a_2\omega - a_0\omega^3\right)\sin\phi + \left(a_1\omega^2 - a_3\right)\cos\phi}{A b_0} \tag{21}$$

$$k_i = \frac{\left(a_3\omega - a_1\omega^3\right)\sin\phi + \left(a_2\omega^2 - a_0\omega^4\right)\cos\phi}{A b_0} + \omega^2 k_d \tag{22}$$

For the specific gain margin (A_{sp}), putting $A = A_{sp}$ and $\phi = 0$ degree in (21) and (22) yields

$$k_p = \frac{a_1\omega^2 - a_3}{A_{sp} b_0} \tag{23}$$

$$k_i = \frac{-a_0\omega^4 + a_2\omega^2}{A_{sp} b_0} + \omega^2 k_d \tag{24}$$

For the specific phase margin (ϕ_{sp}), putting $\phi = \phi_{sp}$ degree and $A = 1\left(0dB\right)$ in (21) and (22) gives

$$k_p = \frac{\left(a_2\omega - a_0\omega^3\right)\sin\phi_{sp} + \left(a_1\omega^2 - a_3\right)\cos\phi_{sp}}{b_0} \tag{25}$$

$$k_i = \frac{\left(a_3\omega - a_1\omega^3\right)\sin\phi_{sp} + \left(a_2\omega^2 - a_0\omega^4\right)\cos\phi_{sp}}{b_0} + \omega^2 k_d \quad (26)$$

3.2 Non-reheated Turbine without Droop Characteristics

The transfer function of the LFC system having non-reheated turbine without droop characteristics is given by (9). By applying the procedure of section 3.1, the values of parameters k_p and k_i will be obtained as follows.

For the specific gain margin (A_{sp}) :

$$k_p = \frac{a_1\omega^2 - 1}{A_{sp} b_0} \quad (27)$$

$$k_i = \frac{-a_0\omega^4 + a_2\omega^2}{A_{sp} b_0} + \omega^2 k_d \quad (28)$$

For the specific phase margin (ϕ_{sp}) degree:

$$k_p = \frac{\left(a_2\omega - a_0\omega^3\right)\sin\phi_{sp} + \left(a_1\omega^2 - 1\right)\cos\phi_{sp}}{b_0} \quad (29)$$

$$k_i = \frac{\left(\omega - a_1\omega^3\right)\sin\phi_{sp} + \left(a_2\omega^2 - a_0\omega^4\right)\cos\phi_{sp}}{b_0} + \omega^2 k_d \quad (30)$$

3.3 Reheated Turbine without Droop Characteristics

The transfer function of the LFC system having reheated turbine without droop characteristics is given by (11). By applying the same procedure of section 3.1, the values of parameters k_p and k_i will be calculated as

For the specific gain margin (A_{sp}) :

$$k_p = \frac{\left(n_0m_1 - n_1m_0\right)\omega^4 + \left(n_1m_2 - n_0m_3\right)\omega^2 - n_1}{A_{sp}\left(n_0^2\omega^2 + n_1^2\right)} \quad (31)$$

$$k_i = \frac{-n_0m_0\omega^6 + \left(n_0m_2 - n_1m_1\right)\omega^4 + \left(n_1m_3 - n_0\right)\omega^2}{A_{sp}\left(n_0^2\omega^2 + n_1^2\right)} + \omega^2 k_d \quad (32)$$

For the specific phase margin (ϕ_{sp}) =45 degree:

$$k_p = \frac{\begin{bmatrix} -n_0m_0\omega^5 + \left(n_0m_1 - n_1m_0\right)\omega^4 \\ +\left(n_0m_2 - n_1m_1\right)\omega^3 + \left(n_1m_2 - n_0m_3\right)\omega^2 \\ +\left(n_1m_3 - n_0\right)\omega - n_1 \end{bmatrix}}{\sqrt{2}\left(n_0^2\omega^2 + n_1^2\right)} \quad (33)$$

$$k_i = \frac{\begin{bmatrix} -n_0m_0\omega^6 + \left(n_1m_0 - n_0m_1\right)\omega^5 \\ +\left(n_0m_2 - n_1m_1\right)\omega^4 + \left(n_0m_3 - n_1m_2\right)\omega^3 \\ +\left(n_1m_3 - n_0\right)\omega^2 + n_1\omega \end{bmatrix}}{\sqrt{2}\left(n_0^2\omega^2 + n_1^2\right)} + \omega^2 k_d \quad (34)$$

3.4 Hydro Turbine without Droop Characteristics

The transfer function of the LFC system having hydro turbine without droop characteristics is given by (13). By applying the same procedure of section 3.1, the values of parameters k_p and k_i will be calculated as follows.

For the specific gain margin (A_{sp}) :

$$k_p = \frac{q_0p_0\omega^4 + \left(q_1p_1 - q_0p_2\right)\omega^2 - q_1}{A_{sp}\left(q_0^2\omega^2 + q_1^2\right)} \quad (35)$$

$$k_i = \frac{\left(q_0p_1 - q_1p_0\right)\omega^4 + \left(q_1p_2 - q_0\right)\omega^2}{A_{sp}\left(q_0^2\omega^2 + q_1^2\right)} + \omega^2 k_d \quad (36)$$

For the specific phase margin (ϕ_{sp}) =45 degree:

$$k_p = \frac{\begin{bmatrix} q_0p_0\omega^4 + \left(q_0p_1 - q_1p_0\right)\omega^3 \\ +\left(q_1p_1 - q_0p_2\right)\omega^2 + \left(q_1p_2 - q_0\right)\omega - q_1 \end{bmatrix}}{\sqrt{2}\left(q_0^2\omega^2 + q_1^2\right)} \quad (37)$$

$$k_i = \frac{\begin{bmatrix} -q_0p_0\omega^5 + \left(q_0p_1 - q_1p_0\right)\omega^4 \\ +\left(q_0p_2 - q_1p_1\right)\omega^3 + \left(q_1p_2 - q_0\right)\omega^2 + q_1\omega \end{bmatrix}}{\sqrt{2}\left(q_0^2\omega^2 + q_1^2\right)} + \omega^2 k_d \quad (38)$$

4. SIMULATION RESULTS

A four area power system is considered for the controller design having different types of turbines. Areas 1, 2, and 3 consist of hydro, reheated type thermal and non-reheated type thermal turbines respectively without droop characteristics whereas area 4 consists of a non-reheated type thermal turbine with droop characteristics. The stability boundary locus (SBL), is a two dimensional plot of k_p versus k_i for a fixed value of k_d as the angular frequency (ω) varies from zero to infinity (Tan et al., 2006). The SBL and the line $k_i = 0$ divides the (k_p , k_i) plane into stable and unstable regions (Sonmez & Ayasun, 2016).

The (SBL) for the specific gain margin, $A_{sp} = 12dB$ (3.9811) , and specific phase margin, $\phi_{sp} = 45\,\text{deg.}$, are plotted for all the four control areas represented in Fig. 2. Using the SBL, the value of PID controller gains k_p and k_i are determined for a fixed value of k_d. In Fig. 2, black and red curves represent the SBL corresponding to the specific gain margin and specific phase margin respectively. The values of k_p and k_i are chosen from the common area bounded by the black and red curves and the $k_i = 0$ axis for a fixed value of k_d to get the stabilizing PID controller. For the simulation, the values of the governor, turbines, and the electric system parameters are taken as follows (Saxena & Hote, 2016). For the control area 1,

$$K_P = 1, \quad T_P = 6, \quad T_G = 0.2, \quad T_W = 4 \quad (39)$$

For the control areas 2, 3, and 4,

$$K_P = 120, \quad T_P = 20, \quad T_G = 0.08, \quad T_T = 0.3, \quad T_R = 4.2, \quad R = 2.4, \quad c = 0.35 \tag{40}$$

The frequency bias factor ($\hat{B}_i$), and synchronizing constants (T_{ij}) have been taken as follows.

$$\hat{B}_i = 0.425; \qquad (i = 1,2,3,4) \tag{41}$$

$$T_{12} = T_{21} = T_{23} = T_{32} = T_{42} = 0.06, \quad T_{14} = T_{24} = T_{34} = T_{41} = 0.07, \quad T_{13} = T_{31} = T_{43} = 0.08 \tag{42}$$

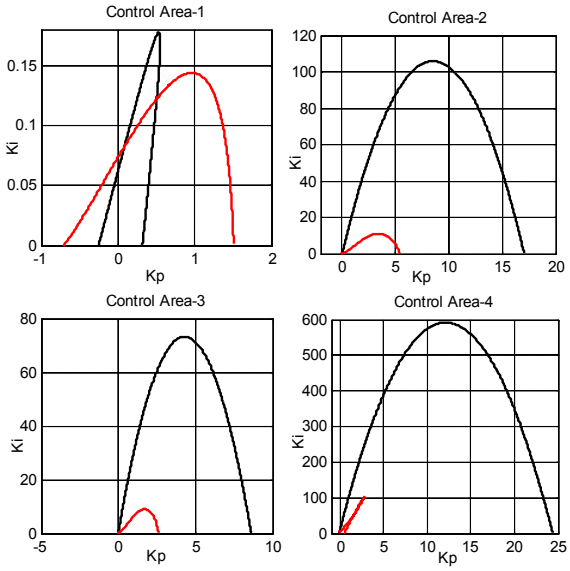

Fig. 2 Stability boundary locus of all control areas

For the control areas 1, 2, 3, and 4, the PID controller gain parameters (k_p, k_i) are selected from Fig. 2 and are given in (43)-(46) respectively. The k_d is kept fixed for drawing each of the four control areas.

$$k_p = 0.3; \quad k_i = 0.06; \quad k_d = 0.8 \tag{43}$$

$$k_p = 1.0; \quad k_i = 0.5; \quad k_d = 1.0 \tag{44}$$

$$k_p = 0.3; \quad k_i = 0.05; \quad k_d = 0.5 \tag{45}$$

$$k_p = 0.05; \quad k_i = 0.1; \quad k_d = 1.5 \tag{46}$$

The Bode plots are obtained from the open loop transfer functions consisting of the above PID controllers $C_i(s)$ and the plant transfer functions $G_i(s)$ of the corresponding control areas. The achieved gain margin and phase margin from these plots are greater than the specific gain margin, $A_{sp} = 12dB\,(3.9811)$, and specific phase margin, $\phi_{sp} = 45\deg$ as given in (47-50). Therefore, the PID controllers obtained by the proposed scheme provide robust stability to the multi-area power system.

$$Area-1: \quad A = 12.3\,dB \quad ; \quad \phi = 67.5\deg \tag{47}$$

$$Area-2: \quad A = Inf\ dB \quad ; \quad \phi = 82.8\deg \tag{48}$$

$$Area-3: \quad A = Inf\ dB \quad ; \quad \phi = 77.1\deg \tag{49}$$

$$Area-4: \quad A = Inf\ dB \quad ; \quad \phi = 45.7\deg \tag{50}$$

Let the control areas 1, 2, 3, and 4 be subjected to a step load disturbance $(\Delta P_{d,i})$ of 0.01 p. u. MW at time instances t =10, 300, 700, and 1100 seconds respectively. Fig. 3 depicts the deviation in frequency in the four control areas in which the frequency deviation (Δf_i) ultimately returns to zero in a very short time. In these figures, the proposed approach in which PID controllers are designed using SBL for specific gain and phase margin is compared with recently developed PID control scheme for four-area power system (Saxena & Hote, 2016) using SBL without specific gain and phase margin. In control areas 1, 2, and 3, the oscillations are less in the proposed scheme while in control area 4, the oscillations are a little more. The settling time in control areas 2, and 4 is lesser in the proposed scheme whereas it is comparable in the control areas 1, and 3.

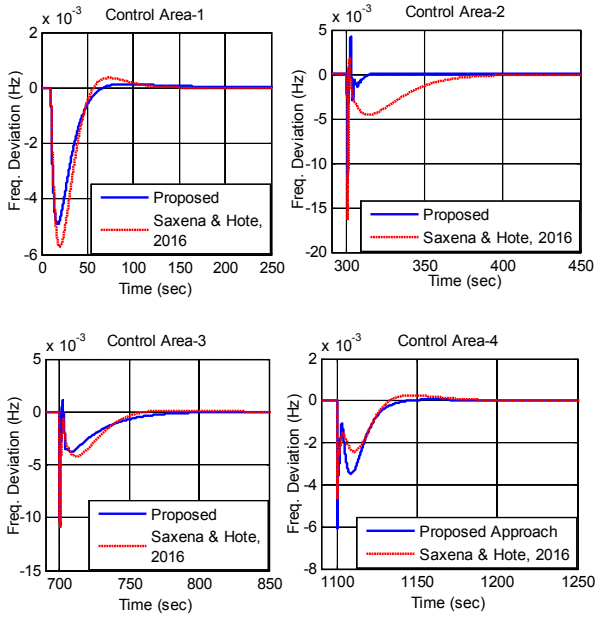

Fig. 3 Frequency deviations in all control areas

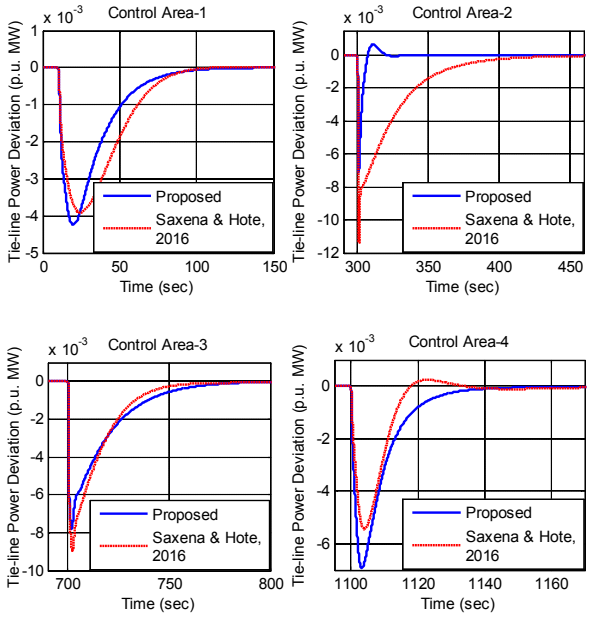

Fig. 4 Tie-line power deviations in all control areas

The net tie-line power deviations, $\Delta P_{tie,i}$, in the four control areas is illustrated in Fig. 4, which shows that tie-line power deviations return to zero in a short duration in all the control areas. Further, a comparison is made with the same methodology as in Fig. 3, and the obtained performance is quite satisfactory. Because of the lack of literature available on the LFC having the same set of turbines as in the proposed method, the comparison is limited to only one technique.

5. CONCLUSION

In this paper, a novel robust PID controller design technique is proposed for the load frequency control problem of four-area power system having different types of turbines. The PID controller gain parameters are determined by utilizing the stability boundary locus methodology. The unique characteristic of the proposed approach is that the SBL are obtained for specific gain and phase margin which ensures robustness to the system. Simulation results illustrate that the proposed technique performs better than the recently reported approach. In future, the proposed method can be applied for LFC problem of a perturbed and nonlinear power system model.

REFERENCES

Anwar, M.N. and Pan, S. (2015). A new PID load frequency controller design method in frequency domain through direct synthesis approach. *Electric Power and Energy Systems*, 67, 560-569.

Cui, Y., Xu, L., Fei, M., and Shen, Y. (2017). Observer based robust integral sliding mode load frequency control for wind power systems. *Control Engineering Practice*, 65, 1-10.

Deniz, F.N., Alagoz, B.B., Tan, N., and Atherton, D.P. (2016). An integer order approximation method based on stability boundary locus for fractional order derivative/integrator operators. *ISA Transactions*, 62, 154-163.

Guha, D., Roy, P.K., and Banerjee, S. (2016). Load frequency control of interconnected power system using grey wolf optimization. *Swarm and Evolutionary Computation*, 27, 97-115.

Hote, Y.V. (2016). PI controller design for one joint robotic arm. In *Proceedings of 14th International Conference on Control, Automation, Robotics & Vision*, Phuket, Thailand.

Hussein, A.A., Salih, S.S., and Ghasm, Y.G. (2017). Implementation of proportional-integral-observer techniques for load frequency control of power system. *Procedia Computer Science*, 109C, 754-762.

Kundur, P. (1994). *Power System Stability and Control*. McGraw Hill, New York.

Padhan, D.G. and Majhi, S. (2013). A new control scheme for PID load frequency controller of single-area and multi-area power systems. *ISA Transactions*, 52, 242-251.

Prasad, S., Purwar, S., and Kishor, N. (2017). Non-linear sliding mode load frequency control in multi-area power system. *Control Engineering Practice*, 61, 81-92.

Qian, D., Tong, S., Liu, H., and Liu, X. (2016). Load frequency control by neural-network-based integral sliding mode for nonlinear power systems with wind turbines. *Neurocomputing*, 173, 875-885.

Sahu, R.K., Panda, S., Biswal, A., and Chandra Sekhar, G.T. (2016). Design and analysis of tilt integral derivative controller with filter for load frequency control of multi-area interconnected power systems. *ISA Transactions*, 61, 251-264.

Saxena, S. and Hote, Y.V. (2013). Load frequency control in power systems via internal model control scheme and model-order reduction. *IEEE Transactions on Power Systems*, 28 (3), 2749-2757.

Saxena, S. and Hote, Y.V. (2016). Decentralized PID load frequency control for perturbed multi-area power systems. *Electrical Power and Energy Systems*, 81, 405-415.

Saxena, S. and Hote, Y.V. (2017). Stabilization of perturbed system via IMC: An application to load frequency control. *Control Engineering Practice*, 64, 61-73.

Shayeghi, H., Jalili, A., and Shayanfar, H.A. (2008). Multi-stage fuzzy load frequency control using PSO. *Energy Conversion and Management*, 49, 2570-2580.

Sondhi, S. and Hote, Y.V. (2016). Fractional order PID controller for perturbed load frequency control using Kharitonov's theorem. *Electrical Power and Energy Systems*, 78, 884-896.

Sonmez, S. and Ayasun, S. (2016). Stability region in the parameter space of PI controller for a single-area load frequency control system with time delay. *IEEE Transactions on Power Systems*, 31 (1), 829-830.

Tan, W. (2009). Tuning of PID load frequency controller for power systems. *Energy Conversion and Management*, 50 (6), 1465-1472.

Tan, W. (2010). Unified tuning of PID load frequency controller for power systems via IMC. *IEEE Transactions on Power Systems*, 25 (1), 341-350.

Tan, N., Kaya, I., Yeroglu, C., and Atherton, D.P. (2006). Computation of stabilizing PI and PID controllers using the stability boundary locus. *Energy Conversion and Management*, 47, 3045-3058.

Tan, W. and Xu, Z. (2009). Robust analysis and design of load frequency controller for power systems. *Electric Power Systems Research*, 79, 846-853.

Vrdoljak, K., Peric, N., and Petrovic, I. (2010). Sliding mode based load-frequency control in power systems. *Electric Power Systems Research*, 80, 514-527.

Zavacka, J., Bakosova, M., and Matejickova, K. (2012). Robust PID controller design for unstable processes with parametric uncertainty. *Procedia Engineering*, 42, 1572-1578.